Journal of
Environmental & Analytical Toxicology

Bahloul, et al., J Environ Anal Toxicol 2015, 5:4
DOI: 10.4172/2161-0525.1000286

Research Article Open Access

Validation of a Laboratory Test Bench for the Efficiency of an N95 Filtering Face Piece, using Simulated Occupational Exposure

Brochot C[1,2], Djebara A[1], Haghighat F[2], Bahloul A[*1]

[1]Chemical and Biological Hazards Prevention, Institute Robert-Sauvé en Santé et Sécurité du Travail, Montréal, Canada
[2]Departments of Building, Civil and Environmental Engineering, Concordia University, Montréal, Canada

Abstract

Ultrafine particles (<100 nm) have special properties that nanotechnologies seek to exploit. However, due to their nanometric scale, these particles can be deposited in the lungs and cause damage. Based on current knowledge, occupational exposure to nanoparticles occurs mainly in workplaces handling nanomaterials, or when certain processes generate them indirectly. However, there are currently no limit values for exposure to ultrafine particles.

To limit worker exposure, respiratory protective devices (RPD) are generally used. The aim of this study was to determine if (a) a laboratory test bench and (b) a simulated occupational exposure setup were reliable representations undesirable exposure in workplace. Thus, two tests benches were used to compare on the one hand conventional measurements and on the other hand sanding- simulation process measurements. NaCl aerosols were generated and then used to measure penetration with constant flow at 43 L/min, 85 L/min and 135 L/min, and one cyclic flow defined by 85 L/min as the mean inhalation flow. The results showed that initial penetrations were less than 5%, as required by the certification. The results also showed that there was a high correlation between the two penetration measurements. One also notes that the measurements had a slightly higher maximum penetration with a charge- neutralized NaCl aerosol than with an un-neutralized NaCl aerosol. The charged-neutralized particles constituted the worst-case scenario exposure.

Keywords: Occupational exposure; Respiratory protective devices; Protection factor; Ultrafine particles; Filtering face piece respirators; Penetration

Introduction

Potential risks associated with ultrafine particles

Nanotechnology is defined as the manufacturing process, the handling, or the study of nanoscale materials. The nanometric scale is defined by standards, and in an approximate range from 1 nm to 100 nm. Nanoscale materials have special properties that nanotechnologies seek to exploit. These properties, a source of many applications and nanotechnologies, can thus be applied to various fields (computers, construction, automotive, aerospace, textiles, cosmetics and drugs). Due to their properties at nanometric scale, nanometer-size particles exhibit different behaviors with materials of the same chemical composition but of larger scale. They may have greater surface reactivity, higher mechanical strength, modified electrical properties, or the ability to penetrate body tissue, etc. But research has shown that nanoparticle properties (size, shape, surface area, charge, chemical properties, solubility, oxidative potential and degree of agglomeration) can influence the toxicity of nanoparticles. Indeed, several studies have shown that, for an equivalent dose by weight, ultrafine particles are insoluble and have more powerful effects than larger particles of similar composition, and can cause noteworthy damage. Regarding air exposure, nanoparticles penetrate the body primarily through inhalation. They are deposited in the lungs and can thus result in certain pulmonary diseases (inflammation, bronchial hyperactivities, acquisition of mutagenicity etc.) and even infect the bloodstream [1].

Occupational exposure in workplaces

There is a considerable gap between the hazard data collected and the occupational exposure limits (OEL) for nanomaterials. In European or USA law, there are currently no limit values for exposure to ultrafine particles. OELs to aerosols are usually defined using two indicators: the mass and the chemical composition of the particles. The exposure limit value of one substance is typically expressed by the mass of particles (solid or liquid) suspended in the air (mg/cm^3), except for fibres where exposures are expressed in number concentration (in $fibres/cm^3$). Exposure to dust, with or without specific nano-effects, is then expressed in mass concentration (mg/m^3). However, risk assessment based only on mass concentration seems irrelevant, because observed effects are not linearly dependent on mass. There is a set of arguments suggesting that, for ultrafine particles, it is preferable to express values by number of particles or total surface area per unit volume. Yet one cannot establish a direct relationship between number of particles and ultrafine particle effects. The nature, specific surface area, structure and chemical composition of the surface of these particles play a key role in potential health effects. Thus, it is necessary to consider each type of particle individually. However, one notes that attempts have been made to derive health-based limit values for frequently used manufactured nanomaterials such as carbon nanotubes [2], fullerenes (C60) [3] and TiO_2 [4].

Based on current knowledge, occupational exposure to ultrafine particles occurs mainly in workplaces using nanomaterials, or when work processes indirectly generate ultrafine particles. The research contained in certain articles (Table 1) has tried to characterize concentrations of ultrafine particles in a variety of workplace activities,

***Corresponding author:** Bahloul A, Chemical and Biological Hazards Prevention, Institute Robert-Sauvé en Santé et Sécurité du Travail, Montréal, Canada, Tel: 514 288-1551; E-mail: bahloul.ali@irsst.qc.ca

Received March 17, 2015; **Accepted** March 31, 2015; **Published** April 04, 2015

Citation: Brochot C, Djebara A, Haghighat F, Bahloul A (2015) Validation of a Laboratory Test Bench for the Efficiency of an N95 Filtering Face Piece, using Simulated Occupational Exposure. J Environ Anal Toxicol 5: 286. doi:10.4172/2161-0525.1000286

though they measured a wide range of exposure levels. These results are highly consistent with certain review articles [5-8]. Welding is one of the most important sources of fine and ultrafine particles in industrial environments, and several studies have investigated the emission characteristics of welding aerosols in workplaces. Occupational exposure to airborne particles may be high, as workers often work close to the source of emissions. These studies [9-12] measured several particle metrics in an attempt to find suitable particle characteristics for use regarding health effects. No current technique facilitates ideal characterization of ultrafine particles generated in a work environment. Each provides useful information on one aspect or another (Table 2). The preferred method is to combine a variety of techniques to characterize the exposure. Particle number is generally a good indicator in the measurement of nano-sized particles. Also, surface area has been proposed as a good indicator of particle toxicity. It is also important to determine the chemical composition of ultrafine particles through the study of their effects on human health. In theory, measurement of particle mass concentration only provides a measure of the amount of micron and sub-micron particles in the air, and is generally not a good measure of ultrafine particles. Nonetheless, it may still be important to measure the mass concentration of large particles and their impact on health. Most instruments commercially available today are not suitable for personal sampling; thus, stationary sampling must be employed in workplaces to monitor and assess exposure to ultrafine particles. For example, a new technique, aerosol mapping, is being employed to assess the spatial distribution of an aerosol in the workplace. This method has been used to assess spatial variability in both particle count and mass concentration [11]. With regard to workplaces, a wide range of particle number concentrations have been reported; these depended on the localisation, instrumentation, and industry. For the most part, size distributions had a geometric mean diameter of between 100 nm and 300 nm. These results were highly consistent with in-laboratory welding simulations [12]. Emissions of ultrafine particles resulted in very high rates (number concentrations higher than 108 particles per cm^3); the

References	Industry - activity	Measurements	Some of the results
Abrams et al.	auto manufacturing	- mass concentration (thoracic)	thoracic mass concentration: 0,13 - 0,56 mg/m^3
Rosenthal and Yeagy	bearing and grinding operations in auto manufacturing	- total mass concentration - particle size distribution (mass)	total mass concentration: 0,486 - 0,770 mg/m^3
Wake et al.	10 industries in UK - Industrial processes involving heat	- particle number concentration - particle size distribution (number)	particle number concentration: (> 5,105 part/cm^3) > ambient level particle size distribution: GMD ≈ 160 nm > GMD (ambient) ≈ 50 nm
Ross et al.	20 small machine shops – {No welding; mean; welding}	- mass concentration (total, PM10)	GM of total mass concentration: {0,15; 0,22; 0,52} GM of thoracic mass concentration: {0,11; 0,17; 0,44}
Peters et al.	an engine machining and assembly facility	- mass concentration (PM1, PM2,5, respirable particles) - particle number concentration	respirable mass concentration: 0,016 - 0,022 mg/m^3 < 300 nm particle number concentration: 1,84.105 - 1,49.106 part./cm^3
Dasch et al.	auto manufacturing -6 diff general motors plants - 5 processes	- total mass concentration (total, PM2,5) - particle number concentration - particle size distribution (mass)	total mass concentration: MOUDI: 0,18 - 1,10 mg/m^3 and filter: 0,070 - 1,1 mg/m^3 PM1,0 concentration: MOUDI: 0,024 - 0,097 mg/m, APS: 0,022 - 0,045 mg/m and DustTrak: 0,11 - 0,28 mg/m^3 particle size distribution: MMAD depends on activity
Evans et al.	an automotive grey iron foundry	(PM1, PM2,5, respirable particles) particle number concentration: - particle number distribution (number and mass)	respirable mass concentration: 0,05 - 0,15 mg/m^3 < 300 nm particle number concentration: 7,01.10 - 2,39.10 part./cm particle size distribution: high concentration in the smallest channel ELPI (0,007 -0,023 µm)
Kaluza et al.	welding fume aerosol in three Swedish workshops	- mass concentration (PM10, respirable particles) - lung deposited surface area concentration - fine, ultrafine and coarse particle size distribution - chemical analysis - TEM analysis	respirable mass concentration: 600 - 3 400 µg/m^3 PM10 concentration for intense activity: 3 000 µg/m3(background < 100 µg/m^3) particle size distribution: unimodal distribution in number concentration: GMD ≈ 100 – 150 nm unimodal distribution in mass concentration: MMAD ≈ 200 – 300 nm

Elihn and Berg	in seven Swedish industrial plants - including welding	- mass concentration (PM10, PM1, respirable particles) - particle number concentration - total particulate surface area concentration - particle size distribution (number)	PM10 concentration: 0,1 - 1,0 mg/m^3 particle number concentration: 20.103 - 130.103 part./cm^3 particle surface area concentration: 50 - 3 800 µm^2/cm^3 particle size distribution: Generally GMD < 100 nm
Evans et al.	carbon nanofibre production	- mass concentration (respirable particles) - particle number concentration - particle surface area concentration - particle size distribution (number) - photoelectric aerosol sensor	respirable mass concentration: < 12 000 µg/m^3 particle number concentration: < 1,2.106 part./cm^3 surface active area concentration: < 1 500 µm/cm^3 particle number size distribution: conc (small part.) > conc (large part.), 105 part./cm^3 < conc < 107 part./cm^3, primary mode: 200 nm - 250 nm and part. from heat traitment: mode ≈ 10 nm
Liu and Hammond	an automobile assembly plant - including welding	- mass concentration (total, PM2,5, respirable particles) - particle number concentration - particle size distribution (number and mass) - chemical analysis	respirable mass concentration: max = 1 330 µg/m^3 particle number concentration: max = 3,6.1011 part./cm^3 particle size distribution: particle number conc.: max = 3,1.109 part./cm^3

Table 1: Non-exhaustive list of characterization concentrations of ultrafine particles in various workplaces.

			Integral measurement		**Particle distribution measurements**	
			Delayed	**Direct**	**Delayed**	**Direct**
	Advantages		- necessary to ensure continuity in professional assessments		- informative measurement and seems relevant with effects of puf in human health	
		Limitations	- spatio-temporal variability not accounted		- what diameter should be measured? - complex instrumentation - results difficult to interpret	
Particle number concentration	- relatively simple to perform	- background noise particles in ambient air can cause difficulties	- sampling + counting with meb or met	- condensation nucleus counter (cpc, p-trak, portacount)		- mobility particle sizer (smps, fmps, dms 50) - diffusion battery - electrical low pressure iimpactor (elpi) - aerodynamic particle sizer (aps)
Particle surface area concentration	- seems relevant with effects of puf in human health	- instrumentation performance are not yet sufficiently known	- sampling + counting with bet	- diffusion charging (nsam, lq1-dc, ead, dc 2000) - pas 2000		
Particle mass concentration	- necessary to ensure continuity in professional assessments	- seems not enough relevant with effects of puf in human health - difficulties as a sensitivity analysis in samplers	- sampling + gravimetric measurement	- particulate matter sampler with microbalance (teom)	- cascade impactor (moudi) - low pressure impactor (lpi) - sampling + selection (filter, cyclone) + gravimetric measurement	- optical particle counter (opc)
Particle shape/ component measurement	- informative measurement	- is it relevant? - how to characterize these particles? - there is no method of stabilized	- sampling + analysis with meb or met or chemical analysis			

Table 2: Parameters characterizing aerosol particles.

results revealed an aerosol consisting of very fine particles (80–95% of the number distribution <100 nm). Be it exposure in a workplace or simulated activities in a laboratory, there are several issues that make comparison of these results difficult. The main issues are: the lack of a harmonized approach to the measurement strategy and instrumental methods; the parameters measured; the range of dimensions used and the procedures for data analysis. In addition, other factors place limits on these comparisons, namely, contributions to measured concentrations from other sources and a lack of information on the limits of detection.

A limited number of studies have been carried out on sanding processes compared to the welding process. No studies were identified in actual workplaces to measure the number concentration of particles generated by this activity. Some studies [13,14] have been conducted on emissions from sanding paint (nanoparticle-based or not) in a small ventilated chamber used for analysis. Koponen et al. [14] measured a large quantity of dust (106 particles per cm^3). Particle-size distribution varies according to the paint used but exhibits the same modal structure in five modes (the first three modes were less than 200 nm and the two other modes were more than 1 micrometer). These values are consistent with the other studies [13,15]. Szymczak et al. quoted by Koponen et al. concluded that the majority of nanoparticles (less than 100 nm) stem from the electric motor [15,14].

Using respiratory protective devices

Respiratory protective devices (RPDs) are generally used in cases where collective ventilation is not possible, or is insufficient. RPD efficiency is very important for the safety and health of workers potentially exposed to ultrafine particles. Depending on the certification, respirators are tested using a quantitative test for measuring protection factors. There are various protection factors and all are based on the principle of measuring the ratio of contaminant concentrations outside the protection device, C_0, to those inside the device, C_i (1). One observes that the protection factor is equal to the inverse of the penetration (P) of the respirator.

In certification tests, the penetration measurement or Nominal Protection Factor (NPF) allows us to obtain respirator efficiency by measuring C_0 and C_i concentrations in favourable conditions governed by standards. Penetrations do not take into account leaks located on the interface between the mask and the face.

$$PF = \frac{C_0}{C_i} = \frac{1}{p} \quad (1)$$

The Assigned Protection Factor (APF) is the level of respiratory protection that a properly functioning respirator or class of respirators would be expected to provide to properly fitted and trained users in the workplace. The APF takes into account all expected sources of facepiece penetration (i.e. face seal penetration, filter penetration, valve leakage). The government or a standards organization determines the APF. In the United States, for example, the NIOSH and the ANSI both typically establish an APF of 10 for half-face, negative-pressure, air-purifying respirators.

The Workplace Protection Factor (WPF) is the level of protection provided in the workplace, under conditions prevailing in that workplace, by a properly selected, fit-tested and functioning respirator, while it is being correctly worn and used. The WPF is a direct measurement of respirator performance capabilities in a specific work environment. It represents the workplace contaminant concentration outside the respirator (C_0) divided by the contaminant concentration inside the respirator (C_i). Concentrations are measured simultaneously and only while the respirator is being properly worn and used during normal work activities. Thus, measuring the WPF is a very time-consuming and expensive process.

The Simulated Workplace Protection Factor (SWPF) is obtained by measuring respirator performance in a laboratory using test exercises designed to simulate work. The SWPF is determined by measuring a test atmosphere concentration outside (C_0) and inside (C_i) a properly functioning, properly worn respirator. The validity of the SWPF as a surrogate for the WPF depends on how well the test exercises represent the work to be done. In short, the SWPF only describes the effectiveness of the respirator in laboratory conditions, and thus restricts access to the certification of these devices, while the protective factor in the workplace, the WPF, attempts to reflect the actual performance of the respirator. Several studies have attempted to find a correlation between different protection-factor indices, mainly for larger particles; however the correlation has been weak [16,17].

No studies have reported on the measurement of the WPF in workplaces where there was significant exposure to ultrafine particles. Some studies of number concentration were performed in work environments in which there were ultrafine particles, but none have measured the concentration within a respiratory protective device. Several studies have attempted to characterize the performance of half-mask respirators in the workplace, using mass-based assessment of the WPF and for a specific compound. They include [18] for benzo(a)pyren, [19] Zhuang et al. for iron particles and Wu et al. [20] for benzene-soluble fractions measuring the concentrations inside and outside, and using a classical personal sampling method. The resulting WPF have a mean of 47, 920 and 2.5, respectively, for [18-20]. There is also a study by Cho et al. [21], in which the authors measured the WPF (number) - in an agricultural environment - of one elastomeric N95 half-mask, as well as one FFR N95 using an optical particle counter (from 0.7 to 10 µm). They found that the WPF with the elastomeric N95 half-mask was greater than the WPF with FFR N95, and that the WPF increased from 100 to 1,000 as the particle size increased.

Filtration theory

Personal protection devices use media to limit worker exposure: the media in these systems capture particles. Studies have been conducted on penetration dependency on the size of the particle, as in the case of filtering facepiece respirators (FFR), and reusable filters whose media are made of fibreglass. The size of the Most Penetrating Particle Size (MPPS) is between 100 nm and 300 nm. These results are in line with studies on media efficiency. Experimental and theoretical studies on ultrafine particle filtration using various media [22-24] show that the filtration efficiency increases when the aerosol size drops to 4 nm, as predicted by filtration theory. However most of the FFR consist of electret filters. Several studies [23,25-27] show that experimental MPPS occurs below 100 nm, which is consistent with theoretical considerations. For mechanical filters, the neutral ultrafine particles are collected through diffusion, interception, and impaction phenomena. When particles are charged and the filter fibres are neutral, an image force is added to the particle-collecting phenomena [28,29,23]. For electret filters, generally used in N95 FFR, fibres are charged, thereby adding collection forces: a polarisation force for neutral particles, or a Coulombic force for charged particles [28,30]. In all cases, these additional electrical forces significantly increase particle capture. The N95 FFR certification is performed using charge- neutralized particles to estimate performance in the worst-case scenario, the maximum

penetration or the minimum efficiency. With 42 CFR 84 certification, FFR are tested using charged-neutralized NaCl aerosol (for FFR classified N) and DOP aerosol (for FFR classified R or P), with an 85 L/min constant flow and up to 200 mg challenge aerosol load. For NaCl aerosol, the particle size is about 0.075 µm for the count median diameter (CMD) and 1.86 for the geometric standard deviation (GSD), while for the DOP aerosol it is about 0.185 µm for the CMD and 1.60 for the GSD. Concentration measurements upstream and downstream are collected with a photometer or equivalent instrumentation, and the ratio gives the PFF penetration. The certification criterion for N95 FFR is as follows: the total initial particle penetration cannot exceed 5%. This penetration does not take into account leaks located on the interface between the mask and the face.

Most studies on N95 FFR for nanoparticles were performed in-laboratory, applying criteria dictated by standards [31] or approximating, as closely as possible, the actual conditions in laboratory measurements taken in a test chamber: respiration simulation [32], simulated leaks [33] and various types of particles [34]. No one has studied a specific activity that might simulate a workplace protection factor. However, Balazy et al. [35] studied the difference between penetrations in two test benches with different sizes (0.096 m^3 and 24.3 m^3 in volume). These comparisons were made for both 30 L/min and 85 L/min inhalation flow rates. The same spectra penetration was observed in both test benches and for the two flow rates. These results indicate that either chamber can be successfully used to predict respirator performances.

The aim of this study is to simulate the activity of sanding processes and measure the efficiency of an N95 filtering facepiece for the exposure. Performance was measured for both a "natural" and a charge-neutralized aerosol - using three constant flow rates and a cyclic flow - for particle sizes ranging from 20 nm to 200 nm. These measurements were then compared to traditional measurements of filtering facepiece efficiency conducted in a test chamber in a laboratory. In the current study, we seek to compare a chamber and an open setup, with a view to predicting N95 FFR performance in the workplace. The purpose is to verify that laboratory tests are representative of a work activity to which workers could be exposed.

Equipment and Methods

The respiratory protective devices tested

The present study used only one model of the commercially available filtering facepiece respirator, and it was certified N95. The cup-shaped N95 FFRs had two straps, a nose-clip, three layers and no exhalation valve. The soft outer layer was made of polypropylene, and had little effect on either the efficiency or the pressure drop in the mask. The inner layer, which was also the shaping layer, was rigid and determined the shape of the mask. A layer of media was mounted between these two layers; this layer facilitated particle filtration. The respirators were not preconditioned, and they were tested "as received". Silicone was used to fully seal the respirators to a manikin headform, so as to avoid leakage. Thus, all the reported values corresponded to filter penetrations alone, and did not take into account any leakages occurring on the interface between the mask and the face. The penetration measurements thus referred to protection factors exclusive of leakages. This simplification allowed us to compare results from the two test benches and facilitated good reproducibility of measurements.

The laboratory test bench

The laboratory test bench (Figure 1) was constructed at the IRSST and allowed measurement of the N95 FFR penetration [32, 36-38]. It consisted of a test chamber in which generated particles were directed toward the front of a Sheffield head equipped with an N95 FFR. The experimental conditions (pressure, humidity, temperature) within the test chamber were constantly controlled. The design of the chamber had a square section (300 mm) and its length allowed us to achieve a high level of uniformity with the challenge aerosol. The filtering facepiece respirator was sealed to a manikin's head to eliminate leakage. Both constant and cyclic flow rate were used to analyse the efficiency of N95 filters. Finally, two sampling probes, one in front of the mask and the other inside the head, made it possible to measure the protection factor for different configurations.

Measurements with a simulated occupational exposure setup

The simulated occupational exposure (Figure 2), too, was constructed at the IRSST. It consisted of a table on which a rotating disc simulated sanding. The NaCl aerosol generator was connected to the table, and six lines of holes just above the rotating disc helped disperse the aerosol. The disk dispersing the generated aerosols was installed at a height of a few millimetres. The manikin head simulated the worker and was placed 23 centimetres in front of the disk, and 27 centimetres above it. The filtering facepiece respirator was also sealed to a manikin's head to eliminate leakage. Both constant and cyclic flow rate were used to analyse the efficiency of N95 filters. Finally, two sampling probes, in front of the mask and inside the head, allowed us to measure the protection factor for different configurations.

The nanoparticle generation system

The particle-generation system in the two setups consisted of a 6-jet collison generator, a drying system and a 85 Kr electrical charge equilibrator (in Figure 1, and in configuration "a" in Figure 2). These devices enabled the production of NaCl ultrafine particles. Figure 3 shows particle size distributions produced in a different setup (4 samples Cu), measured using a Scanning Mobility Particle Sizer (SMPS) (comprised of an electrostatic classifier TSI model 3080 with a long differential mobility analyzer TSI model 3081 and a Condensation Particle Counter TSI model 3775). The NaCl particles measured ranged from 20 nm to 200 nm. Particle penetration was then determined as a function of particle size.

In addition, another aerosol, one that had not been neutralized, was used (see configuration "b" in Figure 2) to simulate an aerosol in a real situation when the simulated workplace penetration has been measured.

The test system

The N95 FFR and the manikin coupled with the respiration device were placed in the chamber (Figure 1) or on the table (Figure 2). Two configurations were tested: one at a constant flow (configuration (1) in Figures 1 and 2) and one based on simulated respiration (configuration (2) in Figures 1 and 2). The constant-flow installation configuration, most commonly used in standardization tests, was obtained using a pump. The penetration measurements were carried out at constant flows of 43 L/min, 85 L/min and 135 L/min, respectively.

The simulated respiration was obtained using a flow/volume simulator (Series 1120; Hans Rudolph Inc., Shawnee, KS, USA) so as to provide a simple model of respiration in a sinusoidal waveform. A three-way valve was used to prevent exhalation flows from returning

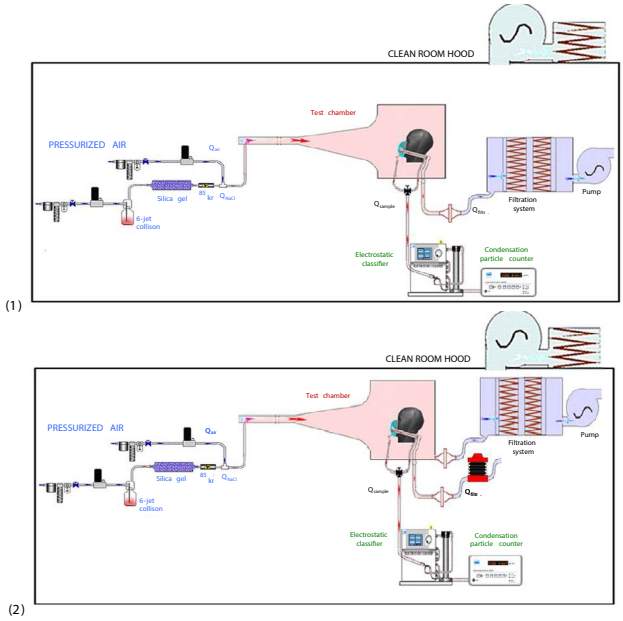

Figure 1: Experimental setup for measuring the protection factor with (1) constant inspiration and (2) a cyclic flow mode.

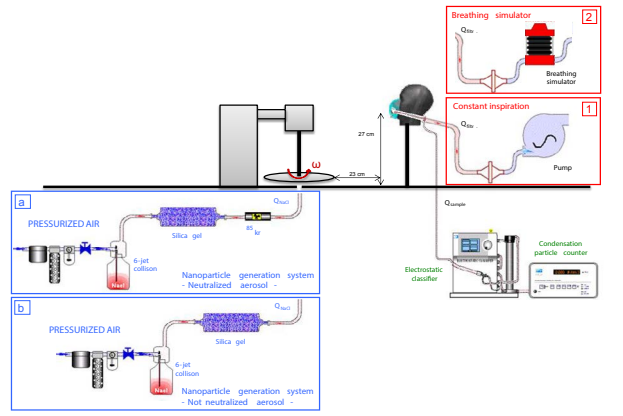

Figure 2: Experimental setup for measuring the simulated protection factor with neutralized aerosol (b) or not (a) and constant inspiration (1) or a cyclic flow mode (2).

via the chamber. Penetration measurements were carried out under one cyclic flow. To obtain an ideal sinusoidal flow, this simulation was performed, respectively, at 42 L/min as the minute volume (Vmin), 85 L/min as the mean inhalation flow (MIF = 2×Vmin) and 135 L/min as the peak inhalation flow (PIF). These choices were made using the NIOSH value (85 L/min, using a constant flow) and drawing on previous studies comparing penetration using constant and cyclic flow rates [39-41,32]. These studies were conducted to compare the performances of N95 FFR using a constant flow and a cyclic flow [39,40,32]. The results showed that the constant flow rate equal to the average breathing (Vmin) underestimated the penetration when compared with the same flow but expressed in cyclic mode; on the other hand, the equivalent maximum cyclic flow (PIF) overestimated the penetration.

The protocol for measuring the N95 FFR protection factor and data analysis

In both setups, aerosols upstream and downstream of the mask were transported using two sampling probes. The two tubes had the same length (about 40-50 cm), so as to obtain the same retention time and the same losses. These aerosols were then selected according to their electrical diameter (using the electrostatic classifier TSI 3080 and the long differential mobility analyzer TSI 3081), while their concentrations were measured using a Condensation Particle Counter (CPC, TSI 3775).

The sampling was collected at the rate of 1.5 L/min and the experimental penetration was obtained from the ratio of the two concentrations in front of the mask, Cu, and inside the head, Cd, as shown in equation (2) below.

$$P = \frac{C_d}{C_u} \quad (2)$$

In the laboratory test bench, each downstream and upstream measurement obtained was the mean of two scans; in the occupational exposure set-up, each downstream and upstream measurement was the mean of six scans; the length of time required by each scan was 315 seconds (300 seconds of measurement and 15 seconds for the DMA voltage adjustment). A measurement taken on the laboratory test bench required more than 10 minutes, and a measurement taken on the occupational exposure test bench required more than 30 minutes. Each measurement was taken twice to verify the generation stability and ensure that the penetration represented a stationary filtration process (i.e. one cannot observe any effect due to clogging); also, four different respirators were tested (N = 4). The penetration values were then analyzed in terms of mean values and standard deviations.

Using NCSS program software (LLC Inc., Kaysville, UT, USA) the comparison tests were performed by analysis of variance (ANOVA) to verify the significance of the test benches and the selected flow rate on the spectrum and the MPPS penetration.

Experimental Protection Factors

Spectral measurements with the different setups

Figures 4-7 show experimental penetrations obtained with both configurations: the laboratory test bench and the simulated occupational exposure setup. The penetration curves exhibit a low penetration and a Most Penetrating Particle Size (MPPS) of <100 nm for electret filters, as predicted by the theoretical simulation of the filtration, and by previous studies. One observes that the penetration results were lower than 5%. These figures also showed that for these filters the MPPS was about 40 nm (between 34 nm and 45 nm), which is consistent with the results of previous studies [23,26-33,35,38]. The filtration efficiency of electret filters depended on the state of the charge on the filter fibres [23]. The results also confirm earlier findings that the penetration of the filtering facepiece increases as one increases the flow rate [23,25,32,37]. These curves show an increase in penetration with an increase in the flow from 43 L/min to 135 L/min. For the laboratory test bench and the simulated occupational exposure setup, one notes that the maximum penetrations measured increased, respectively, from (1.02 ± 0.21)% to (3.00 ± 0.28)% and to (3.40 ± 0.63)% for flow rates from 43 L/min to 85 L/min and to 135 L/min, and from (1.15 ± 0.55)% to (2.77 ± 0.44)% and to (3.86 ± 0.50)%.

As expected, for all tests performed in the present study the filtration

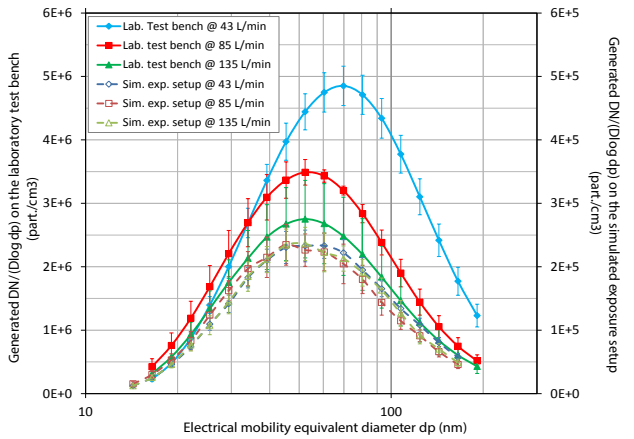

Figure 3: Comparison of particle-size distributions (means and standard deviations, N=4) produced with different conditions in the setup (with neutralization) and in flow rates.

efficiency obtained using N95 revealed that particle penetration through the filter media was independent of particle size distribution, since in both configurations different particle size distributions were used for different setups (Figure 3).

Comparison tests were performed using analysis of variance (ANOVA) to verify the consistency of the comparison of the two configurations. The analysis shows that for a 43 L/min constant flow rate there were no significant differences ($p>0.05$) in penetration measurements obtained with the laboratory test bench and the simulated occupational exposure setup. Regarding the 85 L/min constant flow rate, 44% of the spectrum revealed significant differences in penetration between the two test benches; this difference was 22% for a 135 L/min constant flow rate. This analysis also revealed that the penetration spectra for the cyclic flow rate of the two test benches were totally different.

A more specific analysis of variance on penetration at MPPS revealed that there were no significant differences in these maximum values for the constant flow rates; but the same was not observed for the respiration simulation.

Spectral measurements of the simulated occupational exposure: effects on neutralization

Figures 8-11 show the experimental penetrations obtained from the simulated occupational exposure setup, both with and without neutralization of generated aerosol. In workplaces, the aerosols generated did not necessarily have a charge distribution close to the Boltzmann equilibrium. Here, the aerosol did not go through an alteration charge system in order to get closer to actual working conditions.

As with the previous figures, Figures 8-11 show that, both with and without a neutralized aerosol, the MPPS was about 40 nm, consistent with the results of [35]. One notes, too, that the penetration results were lower than 5%. The curves revealed an increase in penetration, with an increase in flow from 43 L/min to 135 L/min. Note that the maximum penetrations measured decreased slightly from (1.15 ± 0.55)% to (0.86 ± 0.17)% for a 43 L/min flow rate, decreased from (2.77 ± 0.44)% to (1.55 ± 0.84)% for an 85 L/min flow rate, and increased from (3.86 ± 0.50)% to (4.11 ± 0.44)% for a 135 L/min flow rate, respectively, both with and without neutralization in the simulated occupational exposure setup.

Penetrations at 85 L/min, and with a cyclic flow defined by an MIF = 85 L/min, showed the same trend, with a maximum penetration of about 3% with neutralized aerosol, and a maximum penetration of about 1.5 to 2% with non-neutralized aerosol. Consequently, these curves were highly consistent with the previous studies [32,39,40].

Comparison tests were performed using analysis of variance (ANOVA) to verify the significance of the aerosol neutralization

As in the previous comparison, the analysis shows that for a 43 L/min constant flow rate there were no significant differences ($p>0.05$) in the penetration measurements obtained, either with or without neutralization of the aerosol and in the simulated occupational exposure setup. For an 85 L/min constant flow rate, and for the cyclic flow rate (defined by a MIF = 85 L/min), 44% of the spectrum revealed significant differences in penetration; this difference was 33% for a 135 L/min constant flow rate. This analysis revealed an increase in differences in penetration spectra as the flow rate increased.

The more specific analysis of variance of the penetration at MPPS showed that there were significant differences in these maximum values for the 85 L/min constant flow rate and for the cyclic flow rate (defined by a Vmin = 85 L/min). There were no significant differences ($p>0.05$) in these maximum values for the 43 L/min and the 135 L/min constant flow rates.

Discussion

Comparison of the performance of the two configurations

The penetration measurements were made without leakages and allowed us to compare the two test benches: the laboratory test bench and the simulated occupational exposure setup. The results showed that there was a high correlation between the two penetration measurements for both benches in constant conditions [42-45]. The slight difference in penetration increased when the filtration velocity increased, due primarily to the high variability of the N95 FFR. One notes that maximum penetration was not significantly different in constant conditions. This indicates that the laboratory test bench can represent simulated sanding activity reliably. To our knowledge, there are no earlier studies comparing penetration of N95 FFR in the case of a laboratory test bench (conventional measurements) and penetration

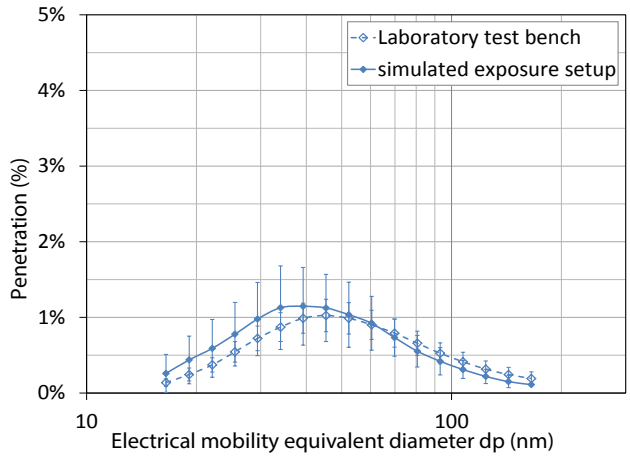

Figure 4: Comparison of penetrations in the two setups and for a 43 LPM inspiration.

in the case of a bench simulating an activity with exposure to ultrafine particles.

The constant flow rate equivalent to the mean inhalation flow (MIF), 2 × Vmin, correctly predicted the effectiveness of the N95 filters. One observes that penetrations at 85 L/min (Figures 5 and 9) and with a cyclic flow defined by a MIF = 85 L/min (Figures 7 and 11) showed the same trend with a maximum penetration of about 3%. These results were highly consistent with the previous studies.

Neutralization of aerosols

N95 FFR certification is performed using charge-neutralized particles to estimate performance in the worst-case scenario, i.e. maximum penetration or minimum efficiency. As shown in the literature review, particle neutralization is even more important when electrets are employed.

Our results are highly consistent with earlier work carried out by [35,30] measured the penetration of an N95 FFR for NaCl particles generated by a 6-jet collison generator, with or without the neutralizer, and at 85 L/min. They observed a significant decrease in penetration without using the neutralizer, which is consistent with the latest theoretical considerations. The Most Penetrating Particle Size measured about 40 nm for neutralized particles. For the setup without neutralization, the MPPS measured had a range of 30 to 60 nm. The maximum penetration then fell from about 5% to about 1.5% between the two different setups. Rengasamy et al. [30] studied the penetration of five N95 FFR for room air particles at 85 L/min. This aerosol was either un-neutralized or charge neutralized. The authors measured the net charge of the two aerosols using an electrometer; these aerosols showed no significant difference in current levels for un-neutralized or neutralized room-air particles. The Most Particle Penetration Size was found to be in the 35-55 nm range for either un-neutralized or charge-neutralized aerosol [46-50]. For three N95 FFR, the maximum penetrations measured were greater for the neutral particles than for the un-neutralized particles, while the maximum penetrations for the other two masks were comparable to one another. These results also revealed that an increase in flow rate increases differences in penetration, both with and without neutralization [51,52].

Conclusions

The aim of this study was to determine if two different benches provided a dependable representation of unfavourable exposures in workplaces. We saw that there was no study measuring the efficiency of N95 FFR in workplaces where workers were exposed to ultrafine particles. Estimating occupational exposure to ultrafine particles in the workplace is already an issue. One substitution method proposed by several agencies (i.e. NIOSH) is to try to simulate a work activity in the laboratory so as to estimate the efficiency of respiratory protective equipment. This method measures the Simulated Workplace Protection Factor (SWPF). In our study, we simulated the sanding activity and measured the efficiency of an N95 FFR. These measures were then compared to conventional measurement of N95 FFR effectiveness in a chamber. The measurements were carried out when the mask was sealed to a manikin.

In the first part, the measurements revealed that all measured penetrations were less than 5%; the certification criterion for N95 specifies that the total initial particle penetration cannot exceed 5%. Furthermore, measurements of penetration were carried out ignoring leakages, with a view to comparing the two test benches. The results showed that there was a high correlation between the penetration

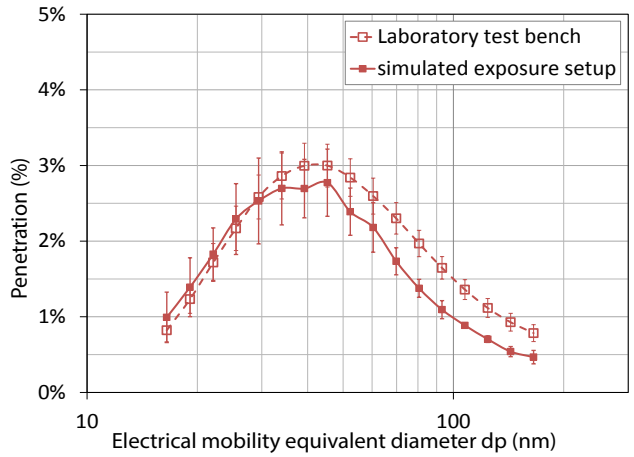

Figure 5: Comparison of penetrations in the two setups and for a 85 LPM inspiration.

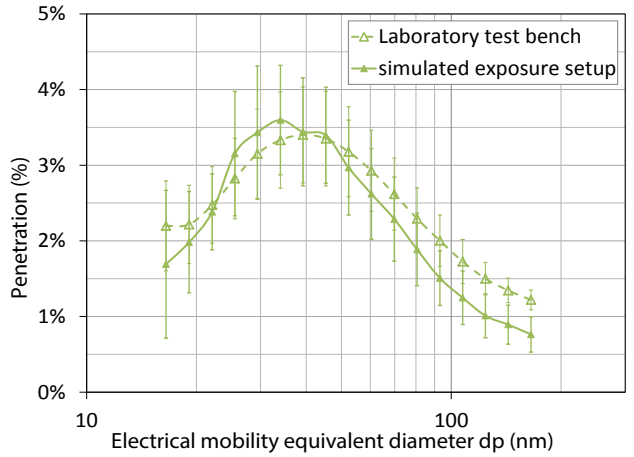

Figure 6: Comparison of penetrations in the two setups and for a 135 LPM inspiration.

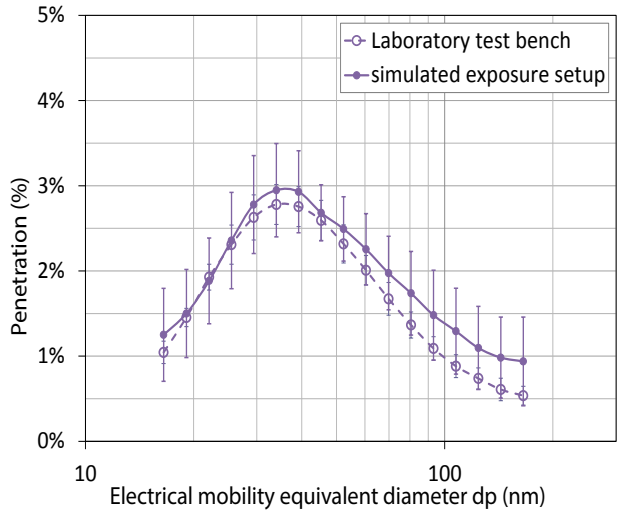

Figure 7: Comparison of penetrations in the two setups and for a cyclic respiration.

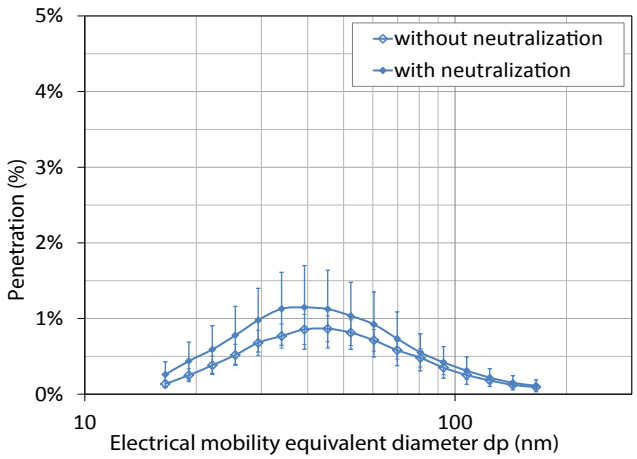

Figure 8: Comparison of penetrations with and without the use of a neutralization source for 43 LPM inspiration.

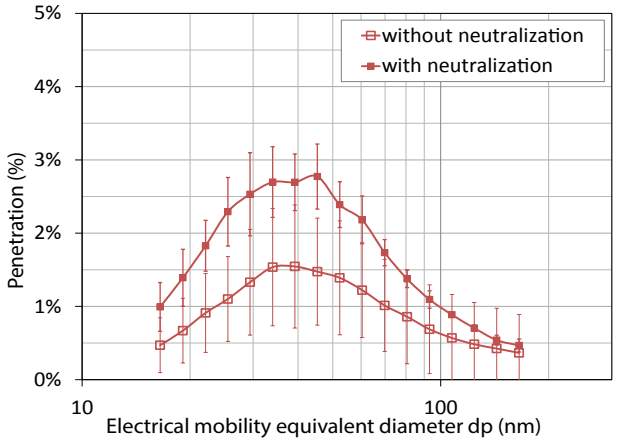

Figure 9: Comparison of penetrations with and without the use of a neutralization source for a 85 LPM inspiration.

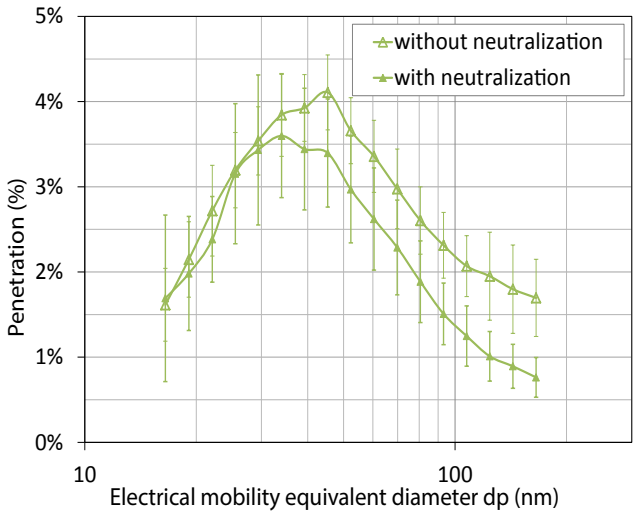

Figure 10: Comparison of penetrations with and without the use of a neutralization source for a 135 LPM inspiration.

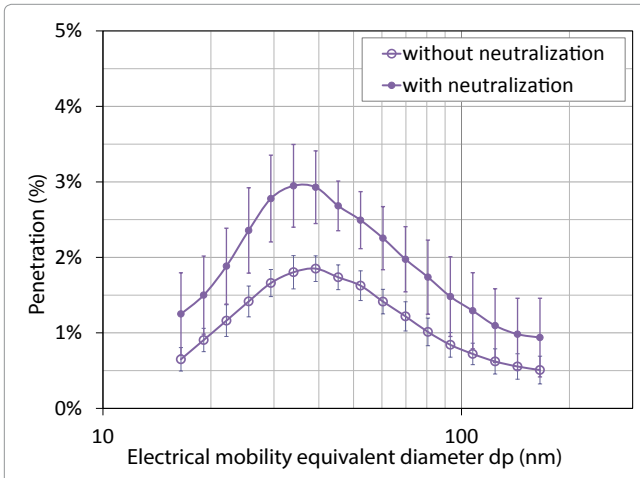

Figure 11: Comparison of penetrations with and without the use of a neutralization source for a cyclic respiration.

measurements involving the laboratory test bench and those involving the simulated occupational exposure setup. One can see that penetration increased when the flow rate increased; however, the maximum penetration measurements were not significantly different at all constant flow rates. Thus, the laboratory bench is a dependable representation of the simulated activity.

In the second part, we measured the effect of aerosol neutralization on penetration via simulated occupational exposure to ultrafine particles in the workplace. The results show that exposure to charge-neutralized particles is the worst-case scenario. There was a slightly higher maximum penetration measured in the case of the charged-neutralized NaCl aerosol. However, we observed that the difference in aerosol charge does not involve any shift in the Most Penetrating Particle Size. In the present article, the MPPS occurred at about 40 nm in all conditions tested.

However, there are certain limitations to this study. In particular, only one N95 FFR was tested for both configurations. Verification is required to determine if one can draw the same conclusions regarding differences in penetration (in terms of neutralized/non-neutralized particles) for different N95 FFR. Also, in order to simplify the setups, the cyclic flow used in this research did not include exhalation; in real life, however, exhalation can affect filter performance.

The use of an N95 FFR without leaks is only the first step in comparing differences between the two benches. That said, this first step allows us to conclude that laboratory tests are representative of the work activity environments to which workers may be exposed. As a follow up, the second step will measure and compare protection factors in a simulated occupational exposure setup and a laboratory test bench.

References

1. Ostiguy C, Soucy B, Lapointe G, Woods C, Ménard L, et al. (2008) Health effects of nanoparticles – Second edition. IRSST Report R-589.
2. NIOSH (2013) Current Intelligence Bulletin 65: Occupational exposure to Carbon Nanotubes and Carbon Nanofibers, DHHS (NIOSH) publication No. 2013-145, Cincinnati, OH.
3. Shinohara N, Gamo M, Nakanishi J (2009) Risk assessment of manufactured nanomaterials –Fullerene (C60), Executive summary.
4. NIOSH (2011) Current Intelligence Bulletin 63: Occupational exposure to Titanium Dioxide, DHHS (NIOSH) publication No. 2011-160, Cincinnati, OH.
5. Schneider T, Jansson A, Jensen KA, Kristjansson V, Luotamo V, et al. (2007)

Evaluation and control of occupational health risks from nanoparticles, Nordic Council of Ministers, Copenhagen: TemaNord 2007: 581.

6. Kaluza S, Balderhaar JK, Orthen B, Honnert B, Jankowska E, et al. (2009) Workplace exposure to nanoparticles, In: Bienko JK (ed), European Agency for Safety and Health at Work (EU-OSHA), Bilbao, Spain.
7. Kuhlbusch TAJ, Asbach C, Fissan H, Gohler D, Stintz M (2011) Nanoparticle exposure at nanotechnology workplaces: A review, Particle and Fibre Toxicology 8: 1-18.
8. Debia M, Beaudry C, Weichenthal S, Tardif R, Dufresne A (2013) Characterization and control of occupational exposure to nanoparticles and ultrafine particles. IRSST Report R-777.
9. Elihn K, Berg P (2009) Ultrafine particle characteristics in seven industrial plants, Annals of Occupational Hygiene 53: 475-484.
10. Isaxon C, Pagels J, Gudmundsson A, Asbach C, John AC, et al. (2009) Characteristics of welding fume aerosol investigated in three Swedish workshops, J Phys: Conf Ser 151: 1-5.
11. Liu S, Hammong SK (2010) Mapping particulate matter at the body weld department in an automobile assembly plant, J of Occup Environ Hyg 7: 593-604.
12. Bémer D, Régnier R, Subra I, Sutter B, Lecler MT, et al. (2010) Ultrafine particles emitted by flame and electric arc guns for thermal spraying of metals, Annals of Occup Hyg 54: 607-614.
13. Choe KT, Trunov M, Grinshpun SA, Willeke K, Harney J, et al. (2000) Particle settling after lead-based paint abatement work and clearance waiting period, AIHAJ 61: 798-807.
14. Koponen IK, Jensen KA, Schneider T (2011) Comparison of dust released from sanding conventional and nanoparticle-doped wall and wood coatings, J Exp Science and Environ Epidemiology, 21: 408–418.
15. Szymczak W, Menzel N, Keck L (2007) Emission of ultrafine copper particles by universal motors controlled by phase angle modulation, J Aerosol Sci 38: 520-531.
16. Coffey CC, Campbell DL, Zhuang Z (1999) Simulated workplace performance of N95 respirators, Am Ind Hyg Assoc J 60: 618-624.
17. Han DH (2002) Correlations between workplace protection factors and fit factors for filtering facepieces in the welding workplace, Ind Health 40: 328-334.
18. Gaboury A, Burd DH, Friar RS (1993) Workplace protection factor evaluation of respiratory protective equipment in a primary aluminum smelter, Applied Occupational and Environmental Hygiene Journal, 8: 19-25.
19. Zhuang ZZ, Coffey CC, Jensen PA, Campbell DL, Lawrence RB, et al. (2003) Correlation between quantitative fit factors and workplace protection factors measured in actual workplace environments at a steel foundry. AIHAJ 64: 730-738.
20. Wu WT (2002) Assessment of the effectiveness of respirator usage in coke oven workers, AIHA J 63: 72-75.
21. Cho KJ, Jones S, Gordon J, McKay R, Grinshpun SA, et al. (2010) Effect of particle size on respiratory protection provided by two types of N95 respirators used in agricultural settings. J Occup Environ Hyg 11: 662-627.
22. Kim S, Harrington MS, Pui DH (2006) Experimental study of nanoparticles penetration through commercial filter media. Journal of Nanoparticle Research 9: 117-125.
23. Huang SH, Chen CW, Chang CP, Lai CY, Chen CC (2007) Penetration of 4.5 nm to 10μm aerosol particles through fibrous filters, Journal of Aerosol Science 38: 719-727.
24. Mouret G, Chazelet S, Thomas D, Bémer D (2011) Discussion about the thermal rebound of nanoparticles. Separation and Purification Technology 78: 125-131.
25. Balazy A, Toivola M, Reponen T, Podgorski A, Zimmer A, et al. (2006) Manikin-based performance evaluation of N95 filtering facepiece respirators challenged with nanoparticles. Annals of Occupational Hygiene 50: 259-269.
26. Rengasamy S, Verboofsky R, King WP, Shaffer RE (2007) Nanoparticle penetration through NIOSH-approved N95 filtering-facepiece respirators, Journal of the International Society for Respiratory Protection 24: 49-59.
27. Rengasamy S, Verboofsky R, King WP, Shaffer RE (2008) Filtration performance of NIOSH- approved N95 and P100 filtering facepiece respirators against 4 to 30 nanometer-size nanoparticles, Journal of Occupational and Environmental Hygiene 5: 556-564.
28. Chen CC, Huang SH (1998) The effects of particle charge on the performance of a filtering facepiece, American Industrial Hygiene Association Journal 59: 227-233.
29. Rengasamy S, Eimer BC, Shaffer RE (2009) Comparison of nanoparticle filtration performance of NIOSH-approved and CE-marked particulate filtering facepiece, Annals of Occupational Hygiene 53: 117-128.
30. Rengasamy S, Miller A, Eimer BC (2011) Evaluation of the filtration performance of NIOSH- approved N95 filtering facepiece respirators by photometric and number-based test methods. Journal of Occupational and Environmental Hygiene 8: 23-30.
31. Code of Federal Regulations (1995) 42 CFR, Part 84, Respiratory Protection Devices, U.S. Government Printing Office, Washington.
32. Mahdavi A, Bahloul A, Haghighat F, Ostiguy C (2014) Contribution of breathing frequency and inhalation flow rate on performance of N95 filtering facepiece respirators, Annals of Occupational Hygiene 58: 195-205.
33. Rengasamy S, Eimer BC (2011) Total Inward Leakage of nanoparticles through filtering facepiece respirators, Annals of Occupational Hygiene 55: 253-263.
34. Cho HW, Yoon CS, Lee JH, Lee SJ, Viner A, et al. (2011) Comparison of pressure drop and filtration efficiency of particulate respirators using welding fumes and sodium chloride, Annals of Occupational Hygiene 55: 666-680.
35. Balazy A, Toivola M, Reponen T, Podgorski A, Zimmer, et al. (2006) Manikin-based performance evaluation of N95 filtering facepiece respirators challenged with nanoparticles. Annals of Occupational Hygiene 50: 259-269.
36. Mostofi R, Wang B, Haghighat F (2010) Performance of mechanical filters and respirators for capturing nanoparticles– limitations and future direction, Industrial Health 48: 296–304.
37. Mostofi R, Bahloul A, Lara J (2011) Investigating of potential affecting factors on performance of N95 respirator, Journal of the International Society for Respiratory Protection 28: 26–39.
38. Bahloul A, Mahdavi A, Haghighat F, Ostiguy C (2014) Evaluation of N95 filtering facepiece respirator efficiency with cyclic and constant flows, Journal of Occupational and Environmental Hygiene 11: 499-508.
39. Richardson AW, Eshbough JP, Hofacre KC (2006) Respirator filter efficiency testing against particulate and biological aerosols under moderate to high flow rates, Edgewood Chemical Biological Center report number ECBC-CR-085. Aberdeen Proving Ground, MD 21010-5424, USA.
40. Haruta H, Honda T, Eninger RM, Reponen T, McKay R, et al. (2008) Experimental and theoretical investigation of the performance of N95 respirator filters against ultrafine aerosol particles tester at constant and cyclic flows, Journal of the International Society for Respiratory Protection 25: 75-88.
41. Brochot C, Michielsen N, Chazelet S, Thomas D (2012) Measurement of protection factor of Respiratory Protective Devices towards nanoparticles, Annals of Occupational Hygiene 56: 595-605.
42. Abrams L, Seixas N, Robins T, Burge H, Muilenberg M, et al. (2000) Characterization of Metalworking Fluid Exposure Indices for a Study of Acute Respiratory Effects, Applied Occupational and Environmental Hygiene 15: 492-502.
43. Cho KJ, Jones S, Gordon J, McKay R, Grinshpun SA, et al. (2010) Effect of particle size on respiratory protection provided by two types of N95 respirators used in agricultural settings. Journal of Occupational and Environmental Hygiene 11: 662-627.
44. Dasch J, D'Arcy J, Gundrum A, Sutherland J, Johnson J, et al. (2005) Characterization of fine particles from machining in automotive plants, Journal of Occupational and Environmental Hygiene 2: 609-25.
45. Evans DE, Heitbrink WA, Slavin TJ, Peters TM (2008) Ultrafine and respirable particles in an automotive grey iron foundry, Annals of Occupational Hygiene 52: 9-21.
46. Evans DE, Bon Ki Ku, Birch ME, Dunn KH (2010) Aerosol Monitoring during Carbon Nanofiber Production: Mobile Direct-Reading Sampling, Annals of Occupational Hygiene 54: 514–531.
47. International Standard ISO/TR 27628 (2008) Workplace atmospheres – ultrafine, nanoparticle and nano-structured aerosols – Inhalation exposure characterization and assessment. Geneva, International Organization for Standardization.

48. Peters TM, Heitbrink WA, Evans DE, Slavin TJ, Maynard AD (2006) The mapping of fine and ultrafine particle concentrations in an engine machining and assembly facility, Annals of Occupational Hygiene 50: 249-57.

49. Peters TM, Elzey S, Johnson R, Park H, Grassian VH, et al. (2009) Airborne monitoring to distinguish engineered nanomaterials from incidental particles for environmental health and safety, Journal of Occupational and Environmental Hygiene 6: 73-81.

50. Rosenthal FS, Yeagy BL (2001) Characterization of metalworking fluid aerosols in bearing grinding operations, American Industrial Hygiene Association Journal 62: 379-82.

51. Ross AS, Teschke K, Brauer M, Kennedy SM (2004) Determinants of Exposure to Metalworking Fluid Aerosol in Small Machine Shops, Annals of Occupational Hygiene 48: 383-391.

52. Wake DD, Mark D, Northage C (2002) Ultrafine Aerosols in the Workplace, Annals of Occupational Hygiene 46: 235-238.